WELDING IN THE WORLD

PEER-REVIEWED SECTION

INTERNATIONAL INSTITUTE OF WELDING
A world of joining experience

HENRY GRANJON PRIZE COMPETITION 2007
Winner – Category C:
"Design and Structural Integrity"
CALCULATION OF THE EFFECT OF TRANSFORMATION EXPANSION ON WELD DISTORTION USING NUMERICAL ANALYSIS

Y. Mikami

ABSTRACT

A numerical simulation considering the transformation effect was applied to the evaluation of the relationship between the martensitic transformation expansion of weld metal and weld distortion of fillet-welded joints. Fillet T-joints were fabricated in order to measure weld distortion and model material properties for numerical simulation. The measured results of weld distortion showed that the weld angular distortion was reduced when low-transformation-temperature welding wire, of which transformation temperature is lower than conventional welding wires, was used. The numerical simulation, considering phase transformation effect, precisely reproduced the measured angular distortion behaviour. The numerical simulation method was applied to the evaluation of the effect of transformation expansion of weld metals on weld distortions of weld joints. The martensitic transformation start or finish temperature was varied in order to clarify the effect of the transformation temperature on weld distortions. Consequently, it was demonstrated that the martensitic transformation start temperature is most effective for reducing weld angular distortion.

IIW-Thesaurus keywords: *Expansion; Deformation; Distortion; Simulating; Transformation.*

1 INTRODUCTION

The construction of structures such as ships and bridges involves fabrication and assembly of individual structural components. The fabrication process requires heating which often includes flame cutting or welding and input of weld-heat causes dimensional changes.

Welding distortion not only interferes with the smooth progress of the fabrication process of steel structures, but also leads to retardation of joint performance, such as buckling strength. Therefore, additional working processes are performed, such as mechanical constraint in order to prevent the generation of distortion, and mechanical bending and line heating to remove welding distortion. However, these additional working processes are costly and time-consuming.

Consequently, a more effective measure for reducing or controlling welding distortions must be developed. From the viewpoint of cost- and time-saving, welding distortion must be controlled in the process of welding and the additional straightening processes must be reduced. One approach that has been studied is to estimate welding

Dr. Yoshiki MIKAMI (mikami@mapse.eng.osaka-u.ac.jp), Osaka University, Graduate School of Engineering, Division of Materials and Manufacturing Science, Osaka (Japan).

Doc. IIW-1859-07 (ex-doc. X-1620r1-07/XIII-2169r1-07), recommended for publication by Commissions X "Structural Performances of Welded Joints – Fracture Avoidance" and XIII "Fatigue of Welded Components and Structures."

distortion by an empirical formula or numerical simulation [1-5], and to use the results to determine appropriate welding conditions for reducing welding distortion. Although numerical simulation of higher accuracy has become available, the results obtained have not been fully utilized in actual fabrication processes.

Recently, other new approaches have been made, utilizing materials with characteristics of phase transformation or strength at elevated temperatures. As is well-known, welding distortion and residual stress of steels are relatively small when the volumetric change due to phase transformation occurs at low temperature. Focusing on this phenomenon, a low-temperature transformation welding wire (LTTW) has been developed [6]. The chemical composition of the welding wire is Ni- and Cr-rich, for the purposes of lowering the martensitic transformation start temperature.

Experiments have shown that using the low-temperature transformation welding wire causes less welding distortion than using conventional wire. However, the relationship between welding distortion and the characteristics of martensitic transformation has not been determined. In order to maximize the effect of the low-temperature transformation welding wire and to use this wire in practical applications, the effect of the transformation and transformation expansion on welding distortion must be clarified. In this study, numerical simulations of welding distortion with varied material properties were conducted in order to determine the required characteristics of the welding wire.

The purpose of this study is to investigate the effect of low-temperature martensitic transformation of weld metals on in-process control of welding distortion. Firstly, fillet T-joints were fabricated in order to confirm the effect of the low-temperature transformation welding wire. Secondly, numerical simulations of the welding distortion of the T-joint were performed, in order to demonstrate that welding distortion could be calculated with high accuracy, by using our developed method. Finally, the numerical simulations were carried out in order to investigate the effect of martensitic transformation start temperature (M_s) on angular distortion.

2 EXPERIMENTAL INVESTIGATION OF WELDED FILLET T-JOINTS

In order to demonstrate the effect of reducing welding distortions, a fillet T-joint was fabricated with the developed low-temperature transformation welding wire. The evolution of angular distortion of the T-joint was measured continuously throughout the welding process and the subsequent cooling process to ambient temperature.

2.1 Configuration of T-joints

The fillet T-joint shown in Figure 1 was fabricated. The steel plate used was a commercial structural steel of 9 mm thickness, which satisfies JIS G 3106 SM490Y. Two different welding wires were used: the conventional welding wire and the developed low-temperature transformation welding wire (LTTW). The conventional welding wire is classified as JIS Z 3313 YFW-C50DM, a commercial welding wire for steel with a required tensile strength of 490 MPa. The low-temperature transformation welding wire has a Ni- and Cr-rich chemical composition to lower the martensitic transformation start temperature. The martensitic transformation start temperature of the welding wire is 205 °C. Chemical compositions of materials used are shown in Table 1. The wire diameter of each welding wire is 1.4 mm.

The rib-plate was fixed on the skin-plate with TIG welding before the main welding procedure. Locations of tack welding are as shown in Figure 1. Both sides of the rib-plate were welded sequentially in opposite directions with 100 % CO_2 arc welding. The interpass temperature between the first and second passes was less than 50 °C. Welding conditions were 300 A – 30.5 V – 45 cpm for the conventional wire and 220 A – 29.5 V – 40 cpm for the LTTW. These conditions were selected in order to achieve a 6 mm leg length of the fillet weld. Throughout the welding process, welded joints were not restrained. Heat treatments, such as preheating or post-weld heat treatment, were not carried out.

2.2 Measurement of temperature profiles and angular distortions

Temperature profiles around welds and displacements of points on the skin-plate were measured continuously during the welding process and the subsequent cooling process.

Temperature profiles were measured by thermocouples located on the top surface of the skin-plate. Figure 2

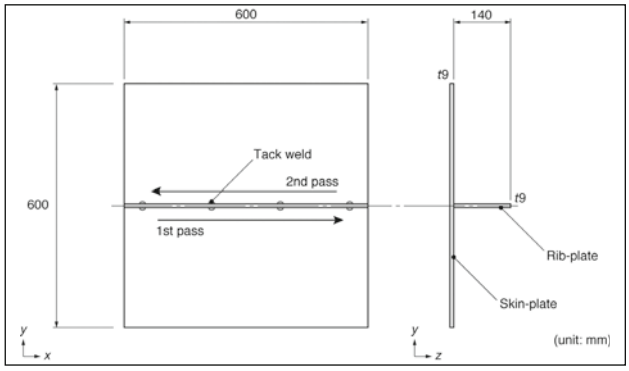

a) Geometry of a T-joint

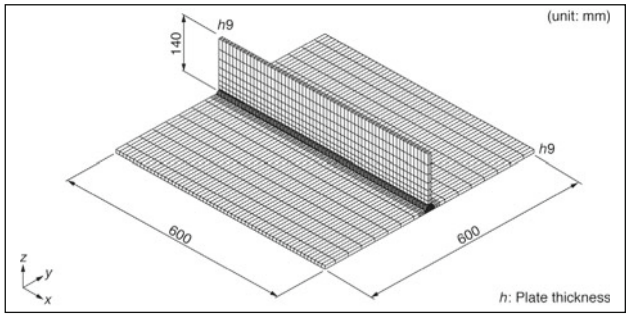

b) Finite element model of a T-joint

Figure 1 – Configuration of a T-joint

Table 1 – Chemical compositions (mass %) of the welding wires and the steel plate

	C	Si	Mn	P	S	Ni	Cr
Low-transformation temperature welding wire	0.020	0.39	0.19	0.010	0.006	10.14	9.76
Conventional welding wire	0.044	0.51	1.59	0.013	0.008	0.01	0.020
Plate steel	0.14	0.28	1.44	0.015	0.004	–	–

shows the locations of the thermocouples. The values shown in Figure 2 indicate distance from the rib-plate. Temperatures measured by thermocouples at points T1 to T6 are denoted T1 to T6, respectively.

Vertical displacements of points on skin-plates were measured by laser displacement sensors. Displacement was measured from the top surface at points D1 to D6 and from the bottom surface at points D7 to D9. The displacement measured at D1 is denoted as d_1 and displacements at the other points are denoted in accordance with this convention.

The T-joint is not restrained, so that the angular distortion occurs asymmetrically as shown in Figure 3. Therefore, the angles between the skin-plate and the horizontal line at both sides were added to evaluate the angular distortion of the T-joint. Calculation of angular distortions considered the displacement of points on the bottom surface of the skin-plate resulting from longitudinal bending. Taking the angular distortion δ_1, the value is calculated from the measured displacements d_1, d_4 and d_7, as illustrated in Figure 3. Angular distortions are calculated at three locations along the welding direction and are denoted δ_1, δ_2 and δ_3, in the order of location from the starting position of the first welding pass.

2.3 Experimental results of angular distortion of T-joints

Figure 4 shows the experimental results of evolution of angular distortion. In the case of the conventional welding wire, the angular distortion levels off after the initial increase. In contrast, in the case of the low-temperature transformation welding wire, the angular distortion starts to decrease after the maximum displacement is reached.

3 NUMERICAL SIMULATION OF WELD DISTORTION OF T-JOINTS

Three-dimensional, finite element analysis was applied to the calculation of weld distortion of the T-joint. SYSWELD [7], a commercial finite element code for welding and heat treatment, was used with transient, non-linear option. The analysis took into consideration the effect

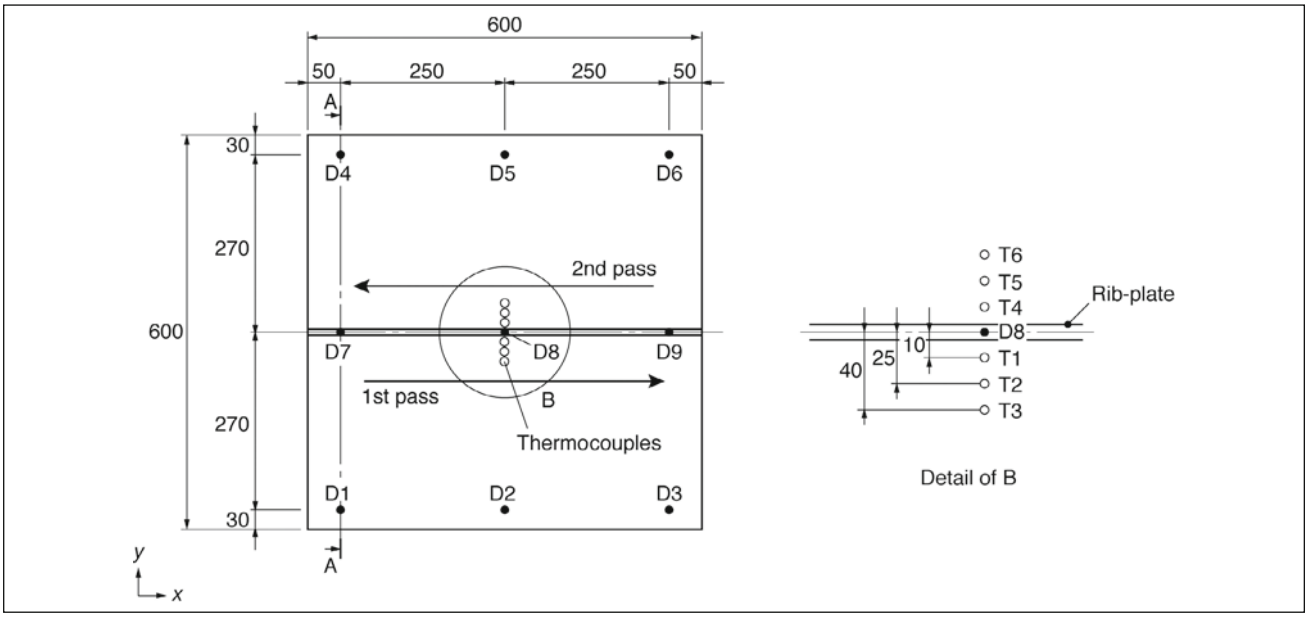

Figure 2 – Location of measuring positions of temperature profile and displacement

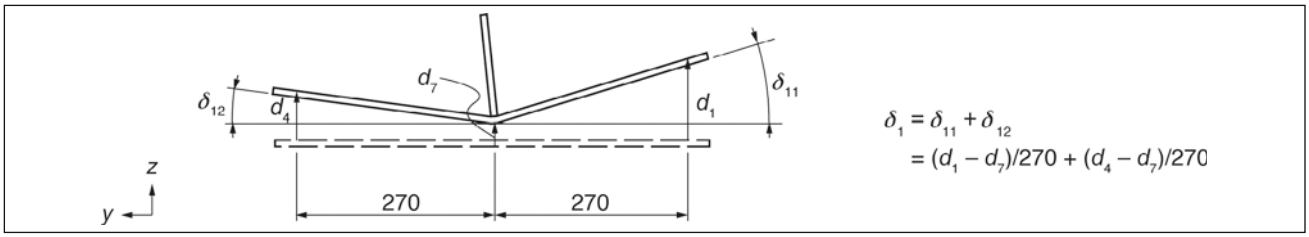

Figure 3 – Definition of angular distortion δ_1 at cross-section A-A in Figure 2

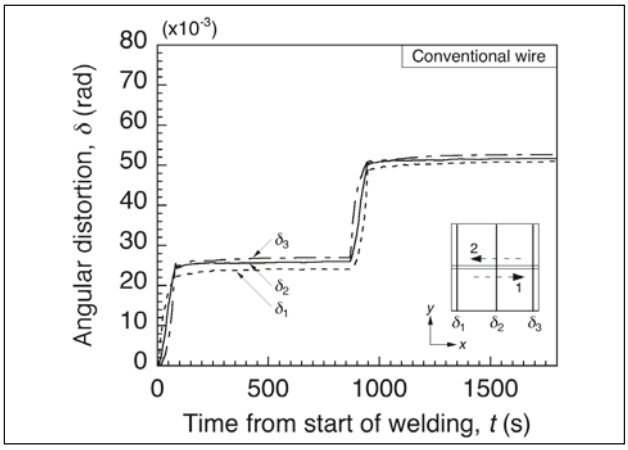

a) Conventional wire

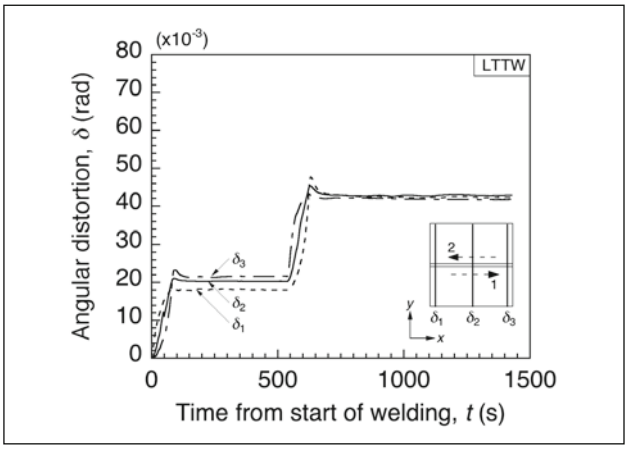

b) Low-transformation temperature welding wire

Figure 4 – Evolution of angular distortion of T-joints

of phase transformation during welding. The numerical simulation was performed in two steps, as follows:

Firstly, weld thermal cycles and the evolution of microstructure were calculated. A heat conduction analysis was performed in order to calculate the weld thermal cycles due to welding, using temperature-dependent material properties. The evolution of the microstructure corresponding to the weld thermal cycle was simultaneously calculated from continuous cooling transformation (CCT) diagrams of the materials used.

Secondly, an elastic-plastic analysis was conducted in order to calculate the transient weld distortions. On the basis of the rule of mixture, the mechanical properties of the materials at arbitrary temperatures during weld thermal cycles were calculated from temperature- and microstructure-dependent mechanical properties, as well as the temperature and fraction of each microstructure obtained by the preceding heat conduction analysis.

3.1 Material properties used in the numerical simulation

Representative material properties used in the numerical simulation were continuous cooling transformation diagrams for the calculation of the microstructural change and thermal expansion/contraction curves, Young's modulus and yield stress for the mechanical calculation. These material properties were measured by simulated weld thermal cycle tests and tensile tests at elevated temperatures. Note that these material properties were measured in specimens extracted from the weld metal of the T-joint, not in the welding wire itself. This is because chemical compositions and consequently mechanical properties of the weld metal of the T-joint differ from those of original welding wire, due to dilution with the steel plate. Table 2 shows the chemical compositions of weld metals. Comparison of Tables 1 and 2 shows that the Ni and Cr content of low-temperature transformation welding wire drops due to dilution with the steel plate.

The evolution of microstructure was calculated from the CCT diagrams shown in Figure 5. The CCT dia-

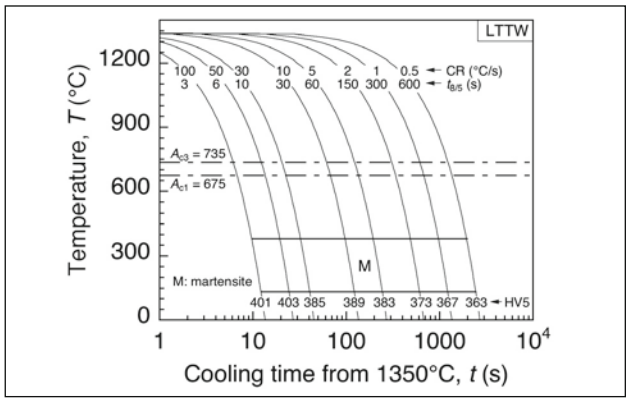

a) Low-transformation temperature welding wire

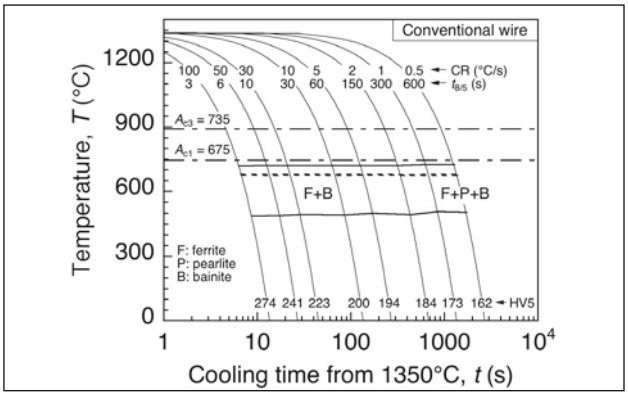

b) Conventional welding wire

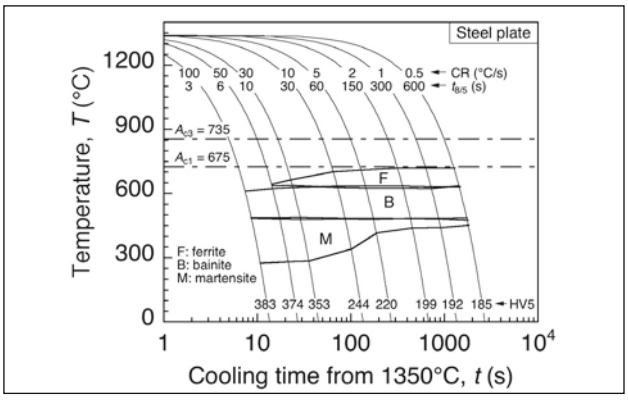

c) Plate steel

Figure 5 – Continuous cooling transformation diagrams

Table 2 – Chemical compositions (mass %) of fillet weld metals the T-joints

	C	Si	Mn	P	S	Ni	Cr
Low-transformation temperature welding wire	0.076	0.43	0.55	0.010	0.006	6.13	6.14
Conventional welding wire	0.10	0.45	1.62	0.013	0.006	0.01	0.01

grams were prepared based on dilatometric test of materials used.

Temperature- and microstructure-dependent yield stresses used in the analysis are shown in Figure 6. The data was measured by a series of high-temperature tensile tests. The thermal expansion/contraction curves of α phase and γ phase for each material are also shown in Figure 6. Examples of dilatometric curves for each material under a heating rate of 10 °C/s and a cooling rate 30 °C/s are also shown in the figure with solid lines.

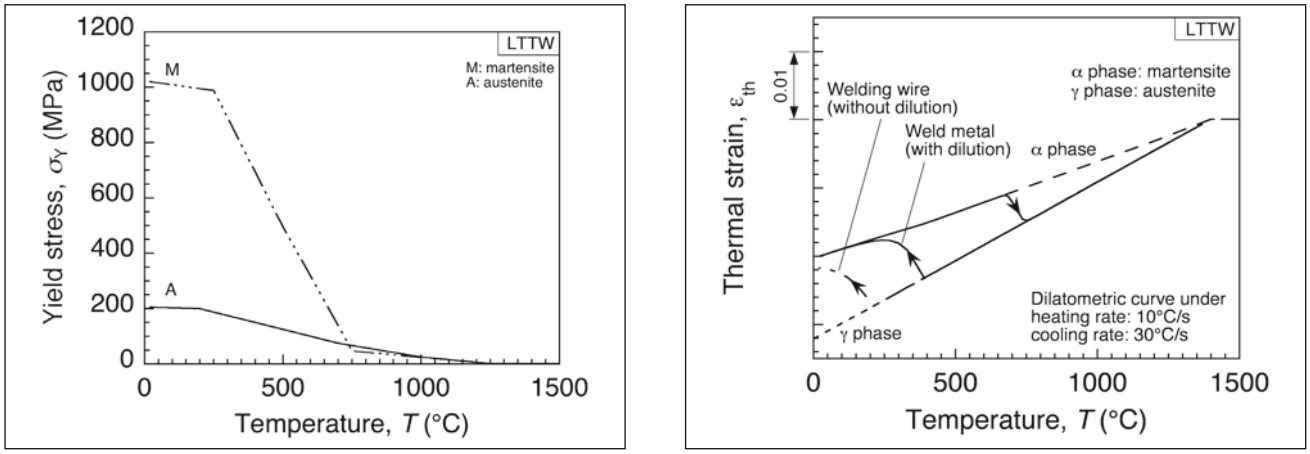

a) Low-transformation temperature welding wire

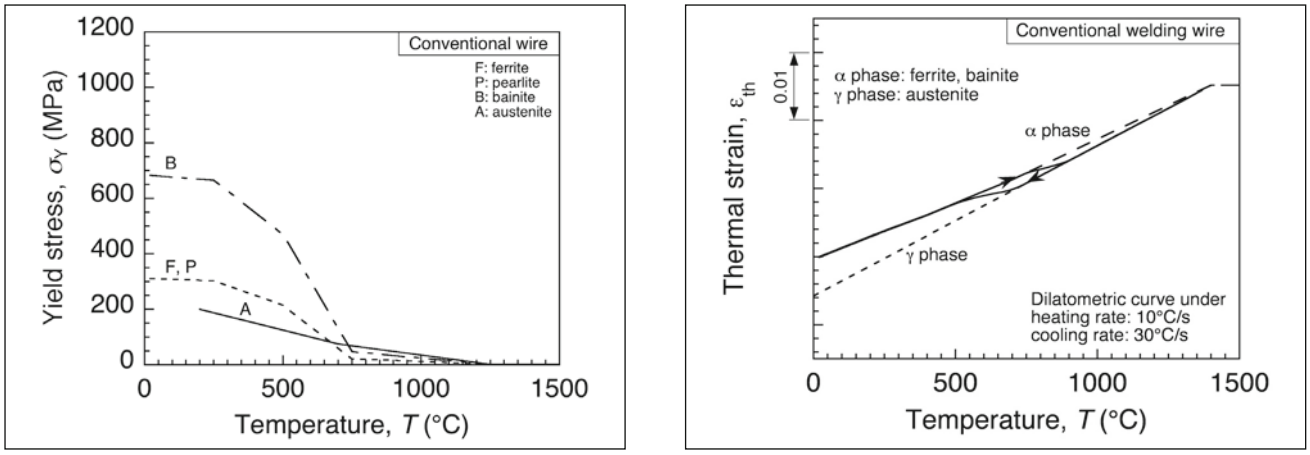

b) Conventional welding wire

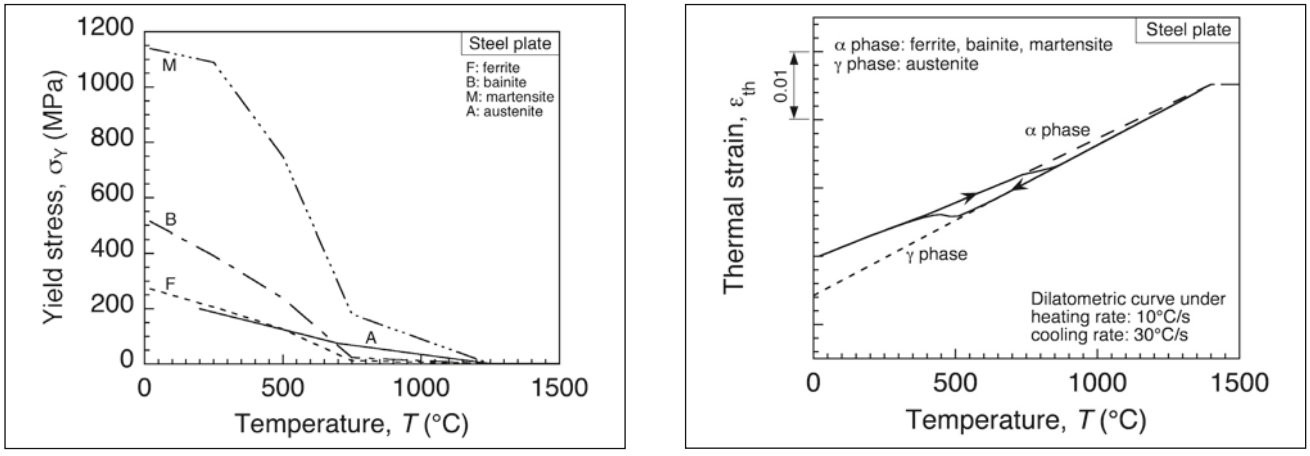

c) Plate steel

Figure 6 – Temperature and microstructure dependency of thermal strain

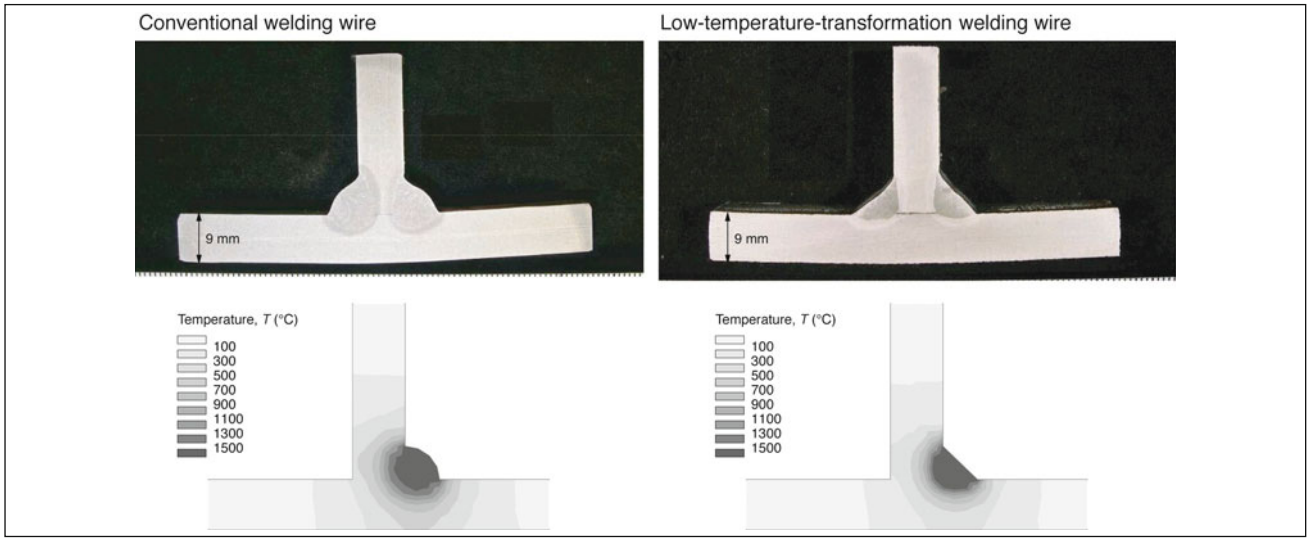

Figure 7 – Cross-sections and isotherms of the welds

For the LTTW, the dilatometric curves of the welding wire itself and diluted weld metal are shown. The martensitic transformation start temperature rises from 205 °C to 380 °C, due to dilution with the steel plate.

3.2 Welding conditions in the numerical simulation

The conditions in the heat conduction analysis were determined by fitting the shape of the fusion zone. Isotherms of the welds obtained by numerical simulations are shown in Figure 7 together with the cross-sections of the welds of T-joints.

3.3 Simulated results of weld distortion of T-joint

Figure 8 shows the evolution of angular distortion during welding as obtained through numerical simulation. The angular distortions of the T-joints with and without the low-temperature martensitic transformation are nicely reproduced. Figure 9 shows a comparison of angular distortions δ_2 between the numerical simulation and the experiment. The angular distortions are calculated with reasonable precision.

Figure 10 shows an enlarged view (0-100 s) of the evolution of angular distortion during the first welding pass in the T-joint with the conventional welding wire. Angular distortion starts to increase in accordance with the distance from the welding start position; δ_1 starts to increase first, then δ_2 and finally δ_3. The numerical simulations are highly accurate for the calculation of not only residual weld distortion, but also distortion behaviour during welding.

In order to clarify the effect of different welding conditions on the distortion, calculation of welding distortion was performed under the same welding condition with different material properties of weld metal. The welding condition is identical to that for LTTW in Figure 8 b) and material properties of weld metal are changed to conventional wire in the numerical simulation. Comparison of angular distortion between LTTW and conventional wire under an identical welding condition is shown in Figure 11. LTTW shows less angular distortion than conventional wire.

3.4 Evaluation of residual stresses

Figure 12 shows the distributions of residual stresses σ_x and σ_y in the transverse direction at the surface of

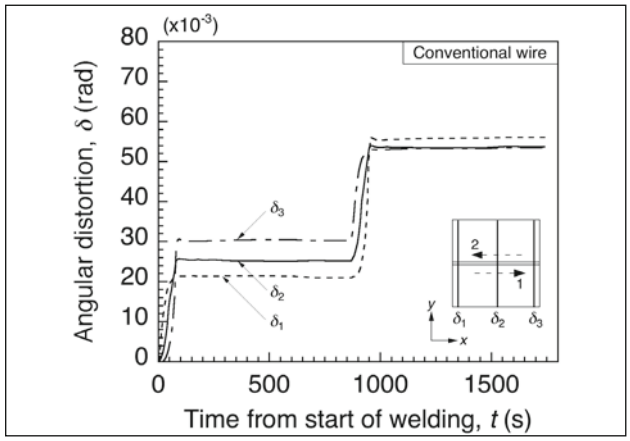

a) Conventional welding wire

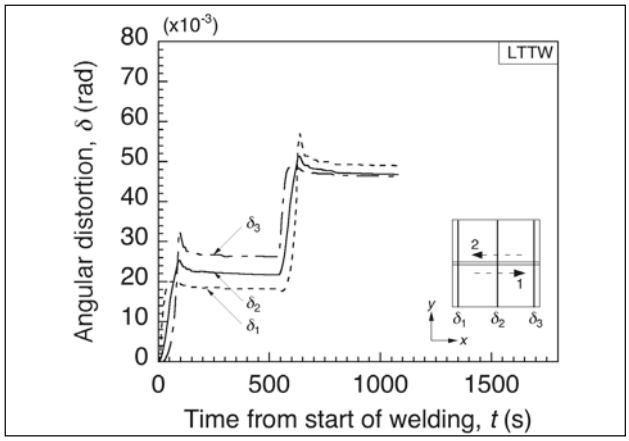

b) Low-transformation temperature welding wire

Figure 8 – Results of numerical simulation of angular distortion

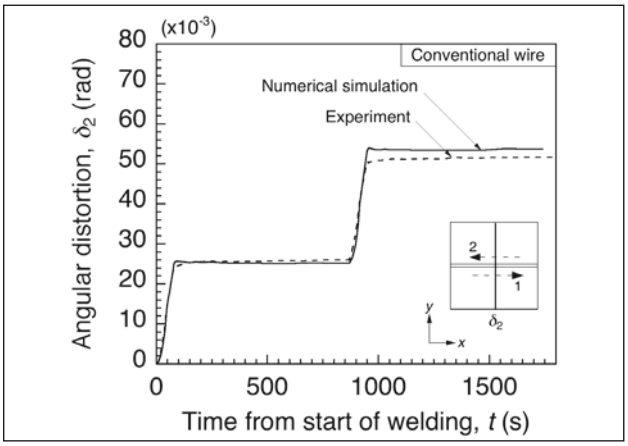

a) Conventional welding wire

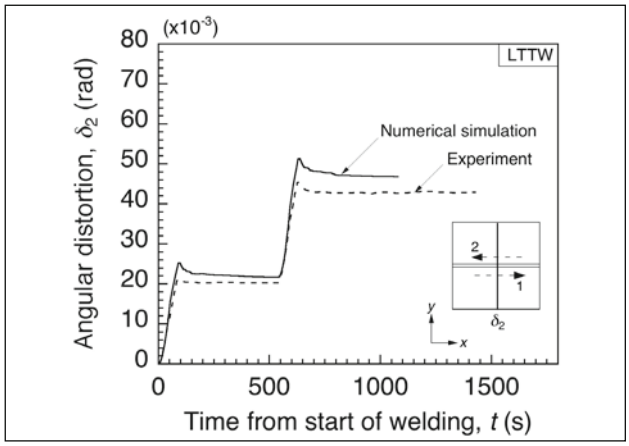

b) Low-transformation temperature welding wire

Figure 9 – Comparison of angular distortion of T-joint between experiment and numerical simulation

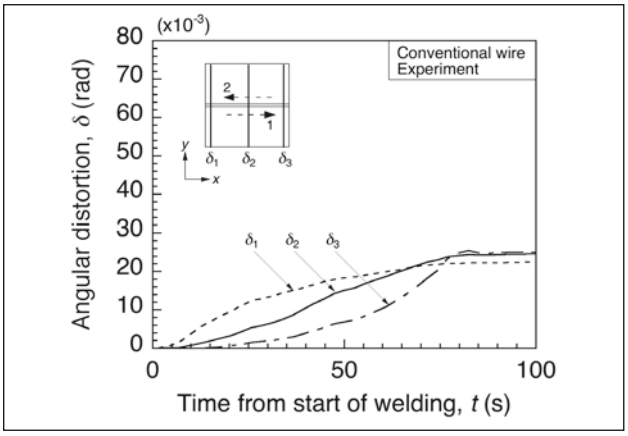

a) Experiment

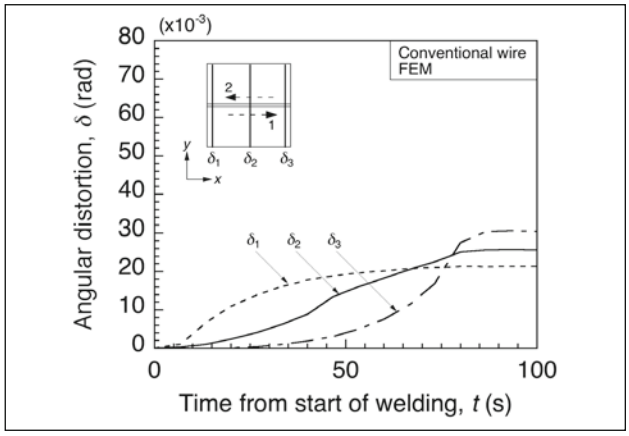

b) Numerical simulation

Figure 10 – Enlarged view of welding distortion during first welding pass

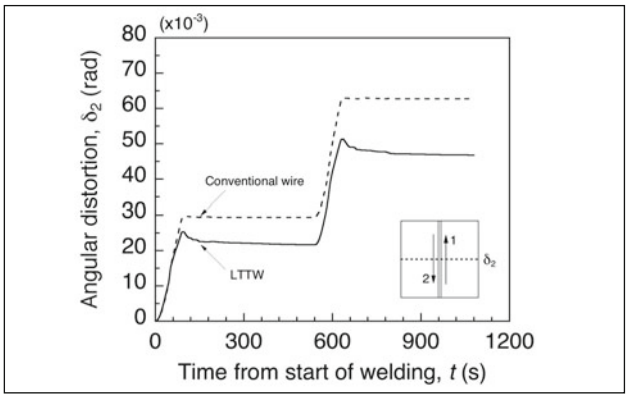

Figure 11 – Comparison of angular distortion under the same welding condition

the plate. As already reported by other researchers [6], residual stresses are lowered with the low-temperature transformation welding wire.

4 EVALUATION OF THE EFFECT OF TRANSFORMATION EXPANSION OF WELD METAL ON ANGULAR DISTORTION

In the preceding section, angular distortion of the T-joints was evaluated by experiments and numerical simulations. The obtained results demonstrate that

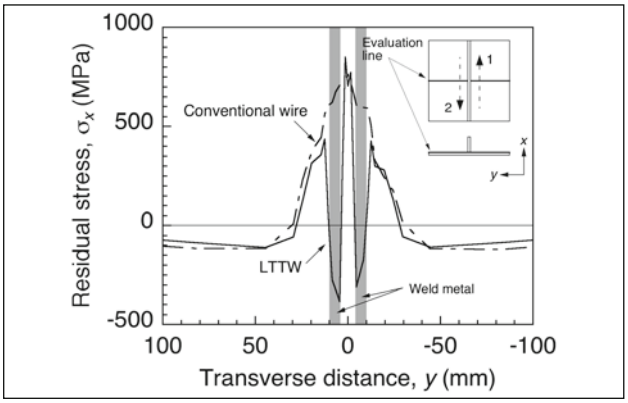

a) Residual stress in welding direction, σ_x

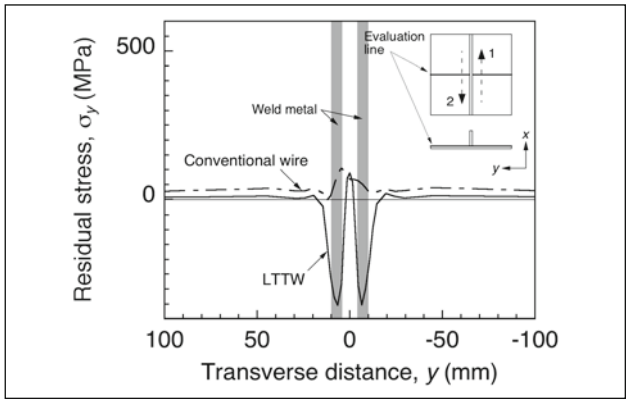

b) Residual stress in transverse direction, σ_y

Figure 12 – Distribution of residual stresses of skin-plate

the low-temperature transformation welding wire is effective for reducing welding distortions. In addition, angular distortion can be calculated with high accuracy by the numerical simulation, considering the effect of phase transformation. However, the effect of the characteristics of martensitic transformation on the angular distortion was not clarified. For effective utilization of the welding wire, the following should also be investigated: the effect of the characteristics of martensitic transformation of the low-temperature transformation welding wire, such as the transformation start or finish temperature and the transformation expansion strain, on the effect of reducing angular distortion. The result would contribute to the development of welding wire that is more effective for reducing angular distortion. In this section, the effect of the martensitic transformation start temperature on angular distortion is investigated.

4.1 Simulation model and material properties

The effect of the martensitic transformation start temperature on angular distortion was investigated with the bead-on-plate welding model shown in Figure 13. The steel plate has the same width and thickness as the skin-plate of the T-joint, but weld length is shortened to 200 mm, in order to reduce calculation time. A single bead was placed on the centre of the plate.

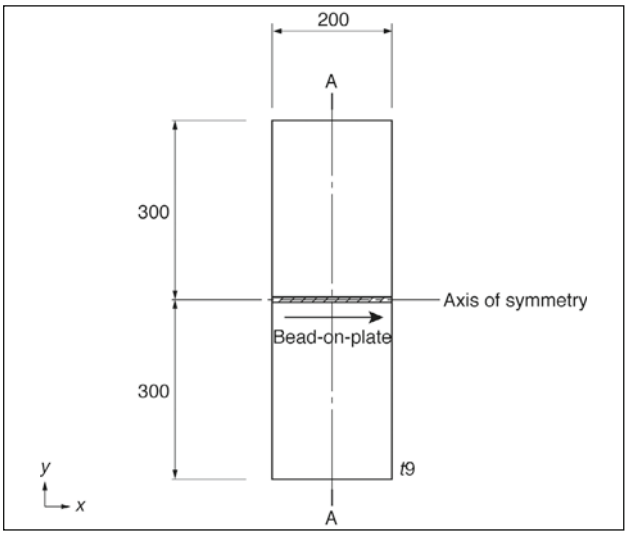

a) Geometry of a bead-on-plate model

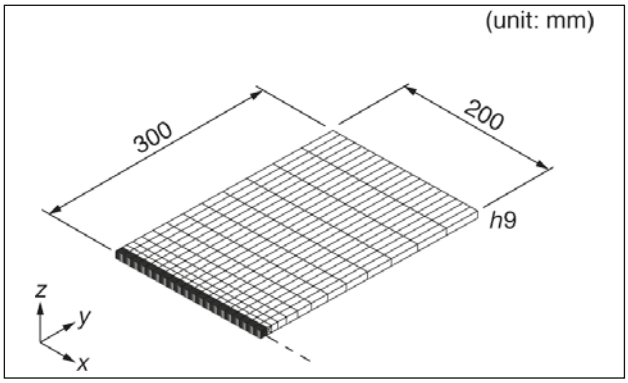

b) Finite element model of a bead-on-plate model

Figure 13 – Configuration of a bead-on-plate model

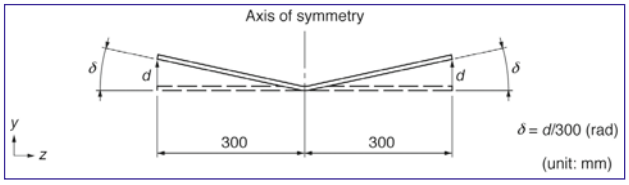

Figure 14 – Definition of angular distortion δ at cross-section A-A in Figure 13

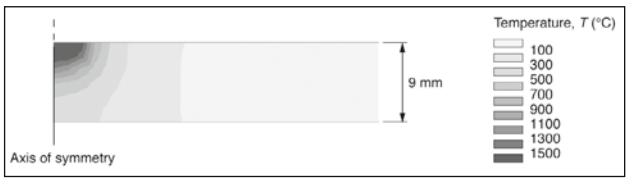

Figure 15 – Isotherms of the welds

The numerical simulation was conducted with half of the plate because of symmetry. Angular distortion was calculated from the vertical displacement of the edge of the plate, as shown in Figure 14. The welding conditions in the numerical simulation were defined to be comparable to those in the T-joint in terms of the depth of the molten area of the skin-plate. The isotherms in the cross-section at the centre along the welding direction are shown in Figure 15. The welding conditions in the numerical simulation are the same as for LTTW and conventional wire.

The material properties used were the same as those used in the numerical simulation of the T-joint, except for the martensitic transformation behaviour of the weld metal. The martensitic transformation start temperature of the weld metal was varied within the range of 405 °C to 0 °C. Figure 16 shows the transformation expansion curves for the weld metal used in the numerical simulation. These transformation expansion curves were obtained by dilatometric tests and were introduced into the numerical simulation, based on Koistinen-Marburger's law to reproduce experimental results. Each material is denoted by its martensitic transformation start temperature, M_s. For instance, "MS380" indicates the weld metal with the martensitic transformation start temperature of 380 °C. Note that the martensitic transformation of materials for which M_s is lower than 205 °C does not end and austenite remains even at room temperature. Angular distortion with conventional welding wire was also calculated.

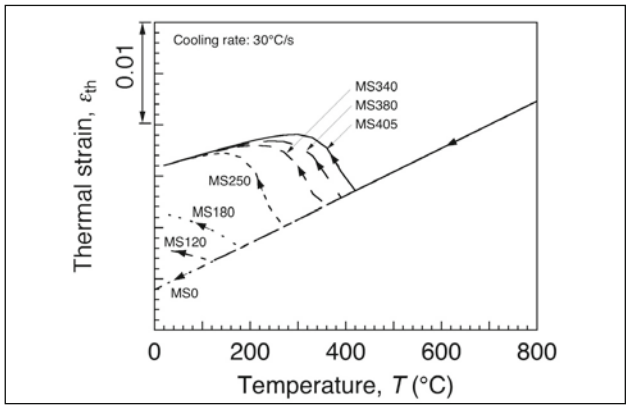

Figure 16 – Dilatometric curves of the weld metal

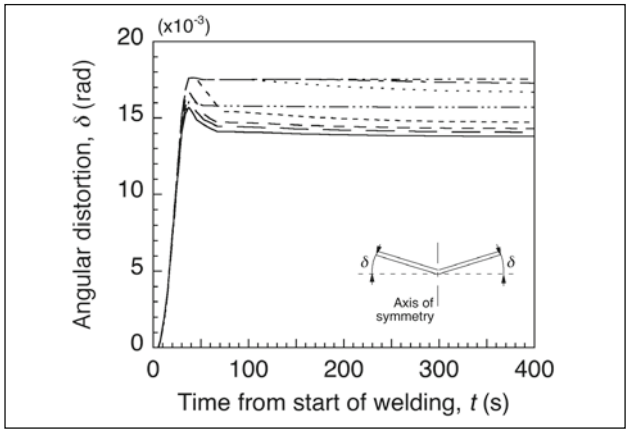

a) Whole history

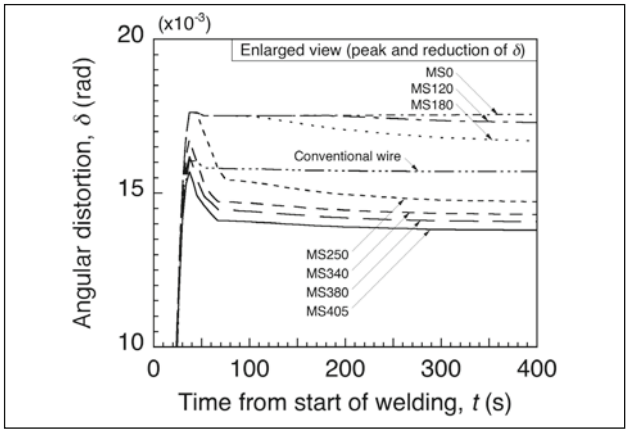

b) Enlarged view

Figure 17 – Angular distortion behaviour of bead-on-plate models with various M_s temperatures

4.2 Distortion behaviour of the bead-on-plate model

Figure 17 shows the evolution of the angular distortion under various transformation expansion curves. Angular distortion starts to increase just after the welding starts. Profiles of angular distortion are almost the same for every M_s temperature, until the angular distortion reaches about 15×10^{-3} rad, after which different behaviour is observed. Until the weld metal reaches to the M_s temperature, the weld metal continues to shrink; therefore, angular distortion continues to increase. When the M_s temperature decreases, shrinkage of the weld metal also increases, so that the peak value of angular distortion increases. Once the weld metal reaches to M_s temperature, transformation expansion occurs; the reduction of angular distortion is observed. Therefore, angular distortion depends on the M_s temperature, as shown in Figure 17. The reduction is also related to transformation expansion strain and the resultant angular distortion is then affected. Consequently, in the cases where the M_s temperature is too low and transformation expansion strain is small, the reduction of angular distortion due to martensitic transformation expansion is not effective: residual angular distortion at room temperature becomes even larger than the conventional wire.

4.3 Relationship between transformation expansion of weld metal and angular distortion

Figure 18 shows, as an example, angular distortion of the bead-on-plate model in the case of MS380. MS380 exhibits the same transformation expansion curve as the developed low-temperature transformation welding wire applied to the T-joint in the preceding section. Figure 18 also shows the case MS0, where the weld metal does not exhibit martensitic transformation expansion.

The reduced angular distortion due to transformation expansion in the case MS380 can be evaluated by comparison with the case of MS0. Figure 19 shows

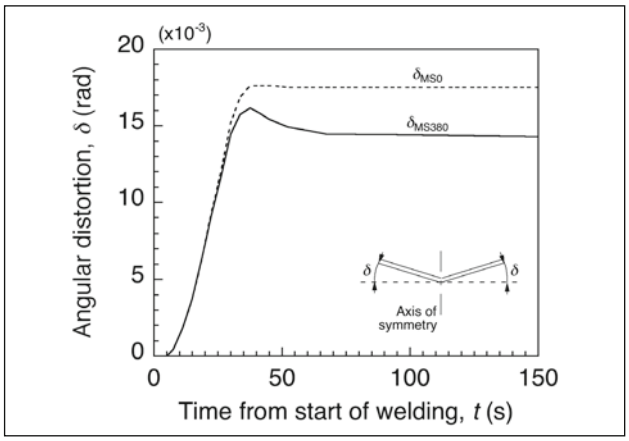

Figure 18 – Comparison of the angular distortion with and without transformation expansion of the weld metal

the difference in angular distortion between MS0 and MS380. In order to investigate the relationship between transformation expansion behaviour of weld metal and angular distortion, transformation expansion curves are plotted in the figure along the time axis, for the starting and ending points of the weld metal in the case of MS380. The transformation expansion curves are obtained from the element located in the centre of the weld metal.

As can be seen from Figure 19, the reduction of the angular distortion starts when the martensitic transformation expansion starts at the welding starting point

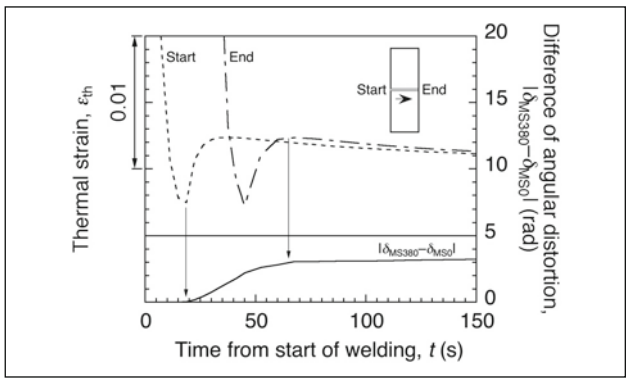

Figure 19 – Relationship between transformation expansion of the weld metal and welding distortion

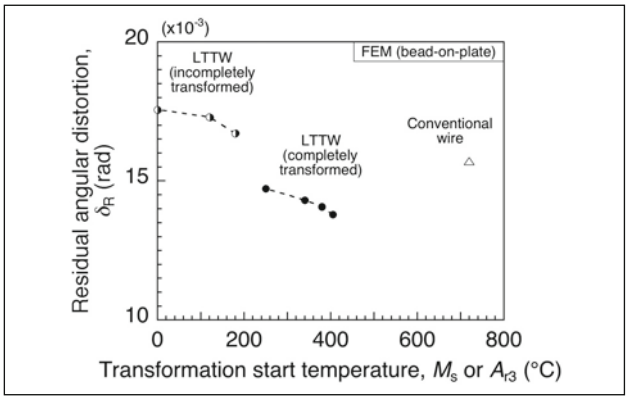

Figure 20 – Relationship between M_s and residual angular distortions of bead-on-plate model

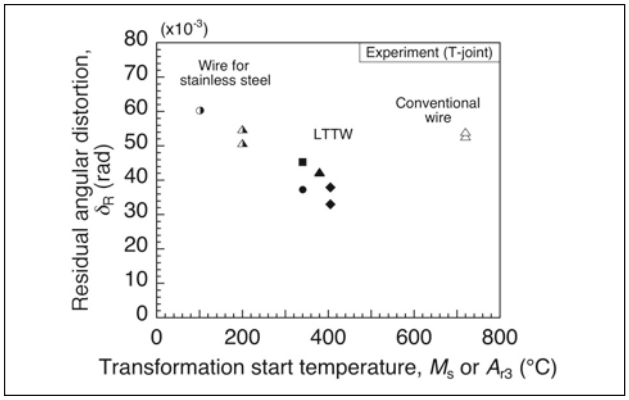

Figure 21 – Relationship between Ms and residual angular distortions of T-joints

and the reduction becomes saturated when the martensitic transformation expansion finishes at the welding ending point. The reduction in angular distortion is directly related to the transformation expansion of the weld metal.

4.4 Effect of martensitic transformation start temperature on angular distortion

Variation in martensitic transformation start temperature leads to differences in behaviours of angular distortions; however, the relationship between the martensitic transformation start temperature and the angular distortion has not been clarified.

In Figure 20, residual angular distortions at room temperature are plotted for the martensitic transformation temperature. For the conventional welding wire, transformation start temperature A_{r3} was selected. The results suggest the existence of an effective start temperature of the martensitic transformation for reducing angular distortion.

Figure 21 shows the experimental results of residual angular distortion of T-joints with welding wires of various martensitic transformation temperatures. Not only the developed wire, but also commercial Ni- and Cr-rich welding wires for stainless steels were used to vary the martensitic transformation start temperature. Different symbols for LTTW and stainless steel wire mean that chemical composition is different. Although the absolute value of angular distortion differs between the experiments of T-joints and the calculation of bead-on-plate model, the minimum value tends to occur at a martensitic transformation temperature of around 400 °C.

5 SUMMARY

Angular distortion of the T-joint was evaluated by experiments and numerical simulations considering the effect of phase transformation. The numerical simulations reproduced, with high accuracy, the behaviour of angular distortion, such as the reduction due to transformation expansion and order of generation of the angular distortion along the welding direction. The relationship between residual angular distortion and martensitic transformation start temperature was investigated with the numerical simulation. The results show that the optimum temperature range for reducing angular distortion exists.

In this study, the effect of the martensitic transformation expansion of weld metals on angular distortion was investigated, with an emphasis on the start temperature of transformation. The effect of other properties, such as transformation expansion strain, could also be evaluated by the same method. The results obtained would be applicable to the materials design of welding wire that is effective for reducing welding distortion.

ACKNOWLEDGEMENTS

The author would like to express his deep gratitude to Professor Masao Toyoda of Osaka University for his considerable guidance for this study.

This research was done under the Japanese national project of the Innovative Technical Programme for Global Warming, Development of Joining Techniques for Steel Structures with Energy Saving, supported by the New Energy and Industrial Technology Development Organization (NEDO) and the Ministry of Economy, Trade and Industries. This work was also supported by the “Priority Assistance for the Formation of World-Renowned Centres of Research – The 21st Century COE Programme (Project: Centre of Excellence for Advanced Structural and Functional Materials Design)” from the Ministry of Education, Sports, Culture, Science and Technology of Japan.

REFERENCES

[1] Ueda Y., Murakawa H.: New trends of research on mechanics in welding and fabrication in Japan, Transactions of Japan Welding Research Institute, 1993, vol. 22, no. 2, pp. 189-200.

[2] Voss O., Decker I., Wohlfahrt H.: Consideration of microstructural transformations in the calculation of residual stresses and distortion of larger weldments, Mathematical Modelling of Weld Phenomena 4 (H. Cerjak, Ed., IOM Communications), 1998, pp. 584-596.

[3] Karkhin V.A., Kreutz W., Pavlova N.O., Schulz W.: Effect of low-temperature phase transformations on residual stress distributions in laser welded joints, Mathematical Modelling of Weld Phenomena 5 (H. Cerjak, Ed., IOM Communications), 2001, pp. 597-614.

[4] Denis S., Gautier E., Simon A., Beck G.: Stress-phase-transformation interactions – Basic principles, modelling, and calculation of internal stresses, Materials Science and Technology, 1985, vol. 1, pp. 805-814.

[5] Karlsson L., Lindgren L.-E., Jonsson M., Josefson L., Oddy A.: Modeling of Residual Stresses and Distortion Development., Mathematical modelling of Weld Phenomena 3, 1997, pp. 571-589.

[6] Ohta A., Watanabe O., Matsuoka K., Siga C., Nishijima S., Maeda Y., Suzuki N., Kubo T: Fatigue strength improvement by using newly developed low transformation temperature welding material, Doc. IIW-1439-98 (ex. Doc. XIII-1706-08), Welding in the World, 1999, vol. 43, no. 6, pp. 38-42.

[7] ESI Group, Ed.: SYSWELD Reference Manual, 2004.